

Holocene climate variability as deduced from the organic carbon and diatom records in the sediments of Lake Aoki, central Japan

*Danda Pani Adhikari,
Fujio Kumon
and Kiyoshi Kawajiri*

地質学雑誌 第108巻 第4号 別刷

2002年4月

THE JOURNAL OF THE GEOLOGICAL SOCIETY OF JAPAN VOL. 108 NO. 4

April 2002

Holocene climate variability as deduced from the organic carbon and diatom records in the sediments of Lake Aoki, central Japan

Danda Pani Adhikari*,
Fujio Kumon**
and Kiyoshi Kawajiri***

Received September 18, 2001.

Accepted February 12, 2002.

* Department of Environmental Sciences,
Faculty of Science, Shinshu University,
Asahi 3-1-1, Matsumoto 390-8621, Japan
Permanent address: Department of Geology,
Tri-Chandra Campus, Tribhuvan University,
PO Box 13644, Kathmandu, Nepal

** Department of Environmental Sciences,
Faculty of Science, Shinshu University,
Asahi 3-1-1, Matsumoto 390-8621, Japan

*** Technical Division, Ueda Factory, Mitsubishi
Mfg. Co. Ltd., Chuo-higashi 5-14, Ueda 386-
8638, Japan

Abstract

In order to understand the climate variability of the Holocene period, two sediment cores were extracted at the northeastern part of Lake Aoki, an intermontane freshwater body located near the northern Japanese Alps, central Japan. The sediments are mainly composed of silty clay with some intercalation of event sediments, including a tephra known as the Kikai-Akahoya (K-Ah) that dates 7,250 cal BP. The sediment chronology yields the sedimentation rate of ca. 0.16 and 0.37 mm yr⁻¹ above and below the tephra, respectively. The sediments were investigated at 0.5 cm interval, providing a time resolution of 13-29 years, for total organic carbon (TOC) and total nitrogen (TN) contents. The record of the organic contents along with the diatom abundance at 50 horizons is used as limnological monitors and climate proxies. The diatom record suggests that the lake has been oligotrophic and alkaline. TOC content and diatom abundance yield close correspondence with both short- and long-term fluctuations, shifting between low- and high-values.

Climate, which control surface-water temperature, appears to be the main factor to affect the variability in the proxy records in Lake Aoki. The climate is dynamic, abruptly switching from various degrees of cool to warm conditions in centennial to millennial scale. Warm conditions prevail from ca. 750-1300, 1750-3050, 4000-5250, 6150-7250, and 8800-10000 cal BP, and cooling occurs during 150-750, 1300-1750, 3050-4000, 5250-6150, and 8350-8800 cal BP. The period between 7250-8350 cal BP is rather fluctuating. Climatic events such as the Little Ice Age (LIA), the Medieval Warm Period (MWP), the Kofun cold stage, and the Holocene Optimum (HOP) are evident, and some other warm and cool events not well recorded before in Japan and abroad are also recognized. The lake also provides a valuable window into the recent climate change and the modern hydraulic changes in the lake system.

Key words: Lake Aoki, organic carbon, oligotrophic lake, diatom, climatic variability, Holocene Optimum

Introduction

A narrow intermontane valley extending N-S from Hakuba to Omachi City near the northern Japanese Alps, central Japan hosts a series of three freshwater bodies, viz. Lake Aoki, Lake Nakatsuna and Lake Kizaki, collectively known as the Nishina Three Lakes (Fig. 1). Beginning of limnological studies of these lakes dates back to 1907 with the work of Tanaka (1930). Yamashita et al. (1985) proposed that the Sano-saka Hill formed by a big landslide dammed the paleo-Himekawa River and created Lake Aoki. Inouchi et al. (1987) drilled two sediment cores bottomed in base-

ment gravel from Lake Aoki in 1987 and the tephra-chronologic age determination of the sediments placed its origin ca. 30 ka BP. The two drilled cores show that the recent sedimentation rate at the sub-basin is much slower than in the main basin. Ono et al. (2000) further discussed the inception mechanism and confirmed the age of Lake Aoki.

Although the Holocene climate history of central Japan has attracted much interest of researchers (e.g., Sakaguchi, 1983; Fukusawa, 1996; Inouchi et al., 1996; Kumon et al., 2000; Adhikari and Kumon, 2001), there still exist much ambiguity in timing and amplitude of climatic events due to the difference in geo-

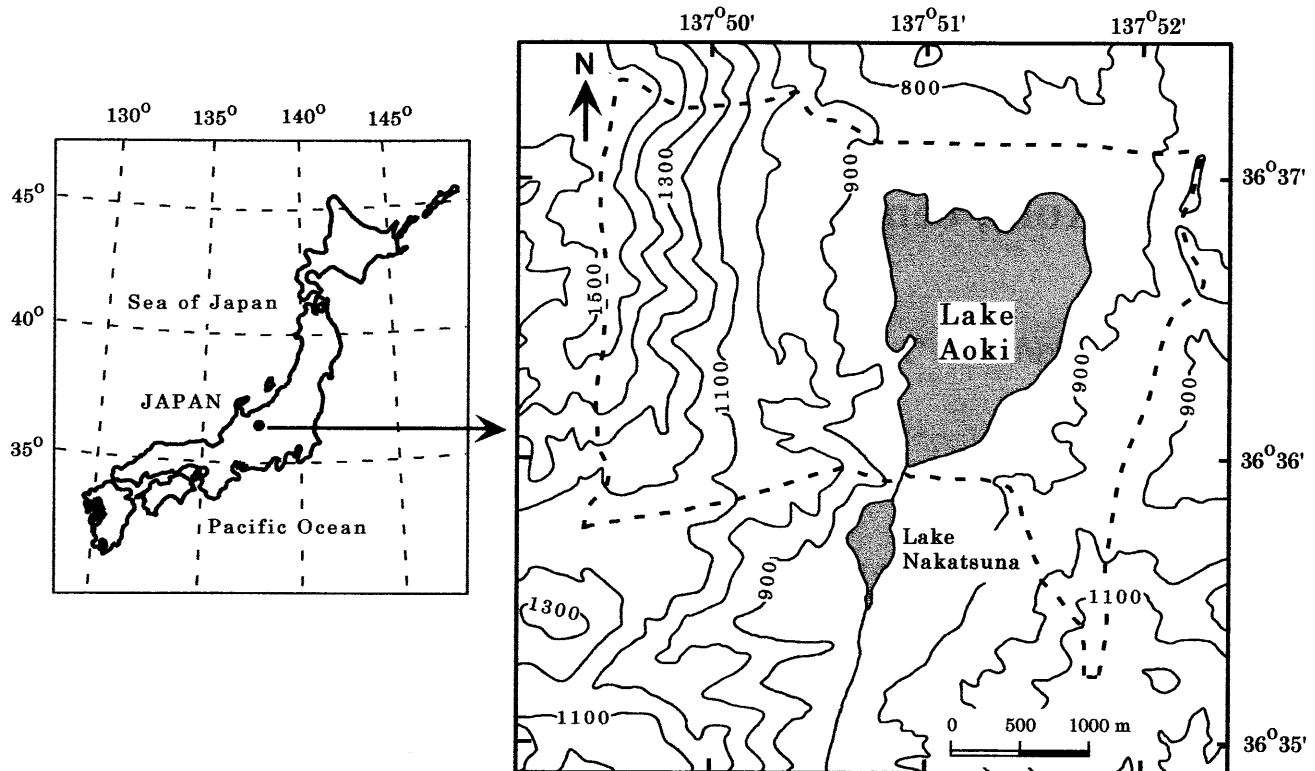


Fig. 1. Location of Lake Aoki and the topographic features around it.

Lake Kizaki and Omachi City are to the south of the map. Dashed line represents watershed boundary. Topographic contours are at 100m intervals (adopted from the topographic map, 1 : 25000, Kamishiro (Geographical Survey Institute of Japan)).

graphical location and methodology used. The long-term (Holocene) archives of sediments from Nishina Three Lakes are unexplored until recently. On a short-term and finer-scale resolution, Kumon (2001) and Adhikari and Kumon (2001) clarified the existence of the Little Ice Age (LIA) and the Medieval Warm Period (MWP) from the sediments of Lake Kizaki and Lake Nakatsuna, respectively.

Even short core from the northern part of Lake Aoki can cover the Holocene period due to the low sedimentation rate. However, studies on the paleoenvironment have not yet been attained for this lake. Further, the lake has some merit that emphasizes the importance of limnological investigation. For example, deep basin with an average depth of 29 m, topographic shelter, short wind fetches, and small tributaries; all contribute for the undisturbed sedimentation and calm environment in the lake. The suitability of the sediment for paleoclimatic study combined with the paucity of long-term paleoclimatic data from the Nishina Three Lakes and the surrounding area promoted our sediment core study from Lake Aoki.

Our main objectives were to understand the modern limnological condition, and to reconstruct centennial to millennial scale qualitative climate change around the lake during the Holocene period and to know its variability. To achieve these goals, high-resolution

records of total organic carbon (TOC) and total nitrogen (TN) contents complemented by its diatom abundance in the core sediments are used as the proxy information. This study provides some of the first records of climate variability in the northern Nagano area and adds to our understanding how dynamic was Holocene climate in the Japanese Islands.

Geographical setting

Some of the geographical and limnological data of Lake Aoki are summarized in Table 1, and the topographic, geologic and meteorologic features are briefly mentioned below. The lake is intermediate in size (1.86 km²), but deepest (58 m) among the Nishina Three Lakes. The drainage basin of the lake is very small compared to the size and the water volume, and the streams draining the catchment are few and small.

Bedrock units in the western part of the lake consist largely of Cretaceous granite and welded tuffs, forming steep slope with maximum altitude of about 1600 m. Tertiary sedimentary rocks (Omine Formation) and Quaternary terrace deposits are distributed in the eastern side of the lake, which has low-lying gentle topography. The hills called Sanosakayama in the northern part of the lake consist of collapse deposits (Yamashita et al., 1985). The Itoigawa-Shizuoka Tectonic Line, a well-known boundary fault, runs throu-

Table 1. Selected geographical and limnological data for Lake Aoki¹

Latitude	36° 36' 32"N
Longitude	137° 51' 14"E
Mean annual temperature (°C)	9.40 ^a
Mean annual precipitation (mm)	2022 ^b
Surface elevation (m)	822
Drainage basin area (km ²)	9.20
In the drainage basin:	
Forest with minor grassland (%)	74.1
Cultivated land (%)	1.4
Residential area etc. (%)	4.2
Lake surface (%)	20.3
Perimeter (km)	6.50
Maximum depth (m)	58
Average depth (m)	29
Volume (× 10 ³ m ³)	53940
Water residence period (days)	193
Maximum relief in the drainage basin (m)	778
Lake type	oligotrophic

¹: location as well as lake and catchment dimensional characteristics were determined from topographic and bathymetric maps, and partly referred from Tanaka (1930), Horie (1962), and Saijo (2001).

^a: at Omachi Meteorological Station (AD 1971-2000), and ^b: at Aoki Power Station (AD 1956-1986).

gh this valley, and the formation of the Nishina Three Lakes may have a genetic relation with this active fault system.

Modern climate is monsoon-type, typified by cold winter and moist hot summer. The northwesterly Asian monsoon wind in winter catches moister from the warm current in the Sea of Japan, and accumulates snow more than 1 m around the lake in every winter, making the mountain slopes suitable for skiing. During winter extremes, peripheral part of the lake sometimes undergoes freezing for a few weeks, but complete ice bounding rarely occurs.

Although the winter precipitation during 1971-2000 period was relatively constant (mean, 290 mm), the summer precipitation varies more and accounts more than a half of the annual amount. A negative correlation exists between total annual precipitation and annual average temperature (Fig. 2), and is particularly apparent between summer precipitation and summer average temperature. Precipitation record is also available at Aoki Power Station beside Lake Aoki for 1956-1986 (Showa Denko Co. Ltd.). The amount for that period varies annually from 1529 to 2623 mm, with an annual average of 2022 mm.

Amount of natural inflow was estimated at 0.023 m⁻³s⁻¹ by Tanaka (1930) and 0.58 m⁻³s⁻¹ by Watanabe et al. (1987). Since 1954, an artificial flow has been supplied from a tributary of the Kashima River for electric power generation at Aoki Power Station, and that joins the lake at its southern extremity close to the outlet sill. This is the largest inflow with an

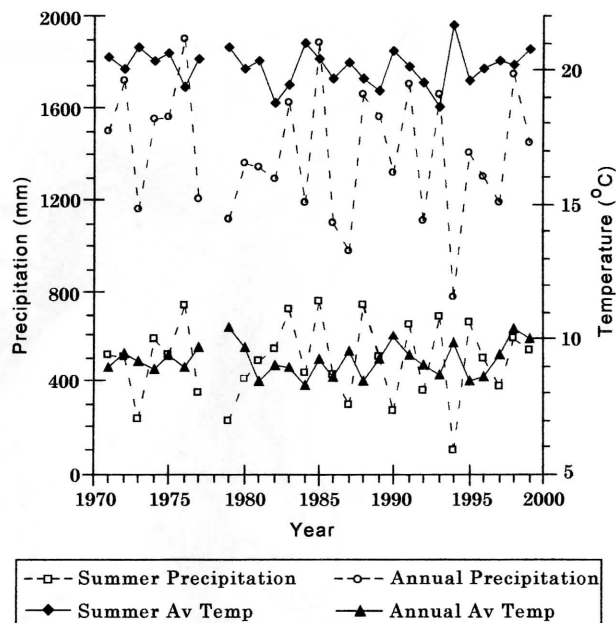


Fig. 2. Variation in temperature and precipitation during AD 1971-2000 at Omachi City, Nagano Prefecture (Data after the Japanese Meteorological Agency).



Fig. 3. Lake Aoki during low water season in early spring off Kakura. Gravel covers coastal area and the finer fractions washed out to the inner lake during the water level lowering.

Muddy sediment distributes abruptly off the gravelly sediment. Staircase-like bedforms are also evident.

annual average volume of 2.69 m⁻³s⁻¹ as of the average of 1974-1987 (Watanabe et al., 1987), and is a few degrees colder than the lake water due to its high altitude origin. Since then, lake water also started to be drained to Tokiwa Power Station through a tunnel for the same purpose. This usage drops lake level during winter and early spring season, with a maximum of 20 m (Fig. 3). Surface outflow from Lake Aoki runs into Lake Nakatsuna to the south through the Upper Nogu River (Fig. 4).

Bathymetry of Lake Aoki defines a main basin and a hanging sub basin, which are separated by a cliff (~

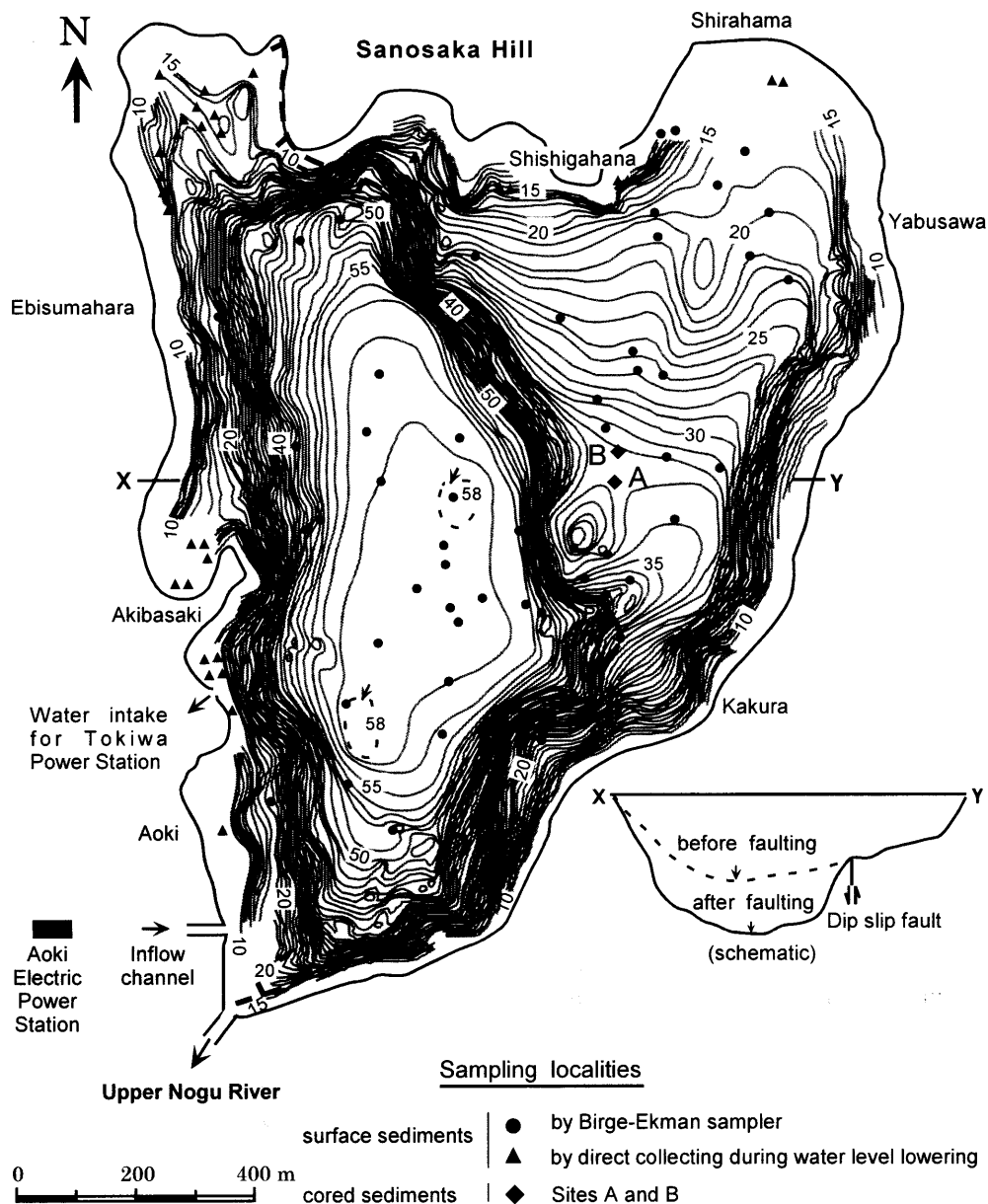


Fig. 4. Bathymetric map of Lake Aoki with the location of sampling sites for the surface and cored sediments. Contours are at 1 m interval. Bathymetric map is redrawn after Inouchi et al. (1987). The dashed thick line with saws indicates the active fault running across the lake (after the Geographical Survey Institute of Japan, 1999). The saws are toward the dip slip side. A schematic cross-section is also shown.

20°) extending NNW-SSE direction (Fig. 4). This cliff is believed to have formed by an active fault running across the lake (Geographical Survey Institute, 1999). The main basin trends NW-SE, shows roughly a rectangular outline, and reaches 55 to 58 m on the basin plain. Steep slopes (15°-20°) bound it to the north, south and west, and gentle foot slope is developed in the northern and southern margin of the basin plain. Besides these features, two dozens of isolated underwater hillocks are distributed in places.

The north eastern one-third of the lake appears gently sloping southwestward (2°-4°) with a small flat area lying under the water depth of about 32 m and

abutting one of the bathymetric highs in the south. This is the sub-basin that is bounded by high gradient (~15°) to the east and south (Fig. 4).

Materials and methods

Bottom surface sediments of about the top 5 cm were collected at 108 locations using Birge-Ekman grab sampler or by direct collecting from the upper slopes during water level lowering (Fig. 4). Sediments were then analyzed for their grain-size using the hydrometer method as mentioned in Kumon et al. (1993).

A 2.25 m long sediment core was extracted from the central part of the sub basin at 32 m depth using a

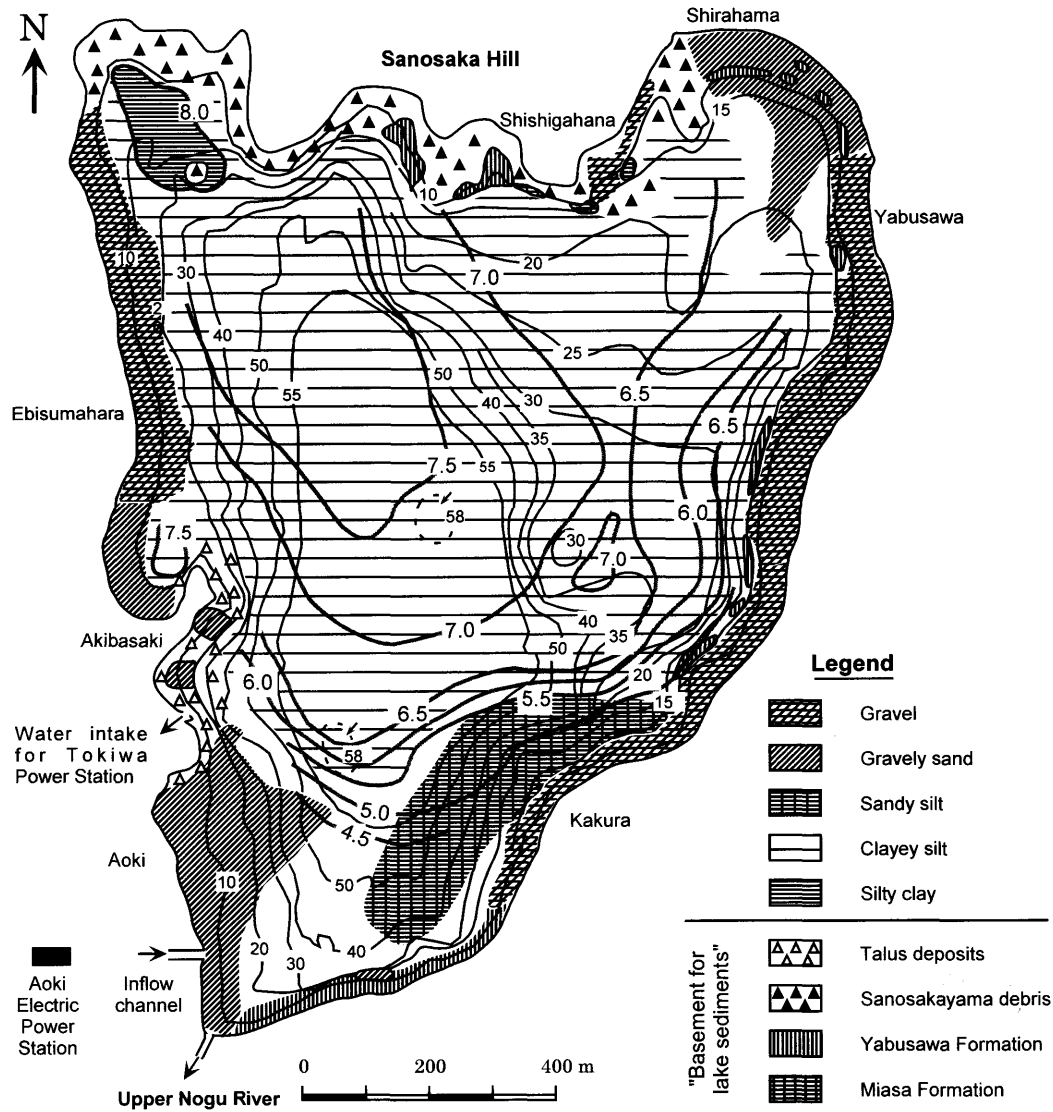


Fig. 5. Distribution of surface sediments in Lake Aoki. The thicker lines labeled with the numbers from 4.5 to 8.0 are median diameter contours in phi scale redrawn (after Kawajiri and Kumon, 1988).

Mackereth piston core sampler (Natsuharagiken Co., Inc.) in September 2000 (Fig. 4, Site A). The core recovered was split lengthwise in laboratory, and lithology was described on the cut surface, with color assignment using Munsell soil color charts. X-ray photograph was also taken to reveal internal sedimentary structures. Sediments were then sub-sampled at 0.5 cm intervals for physical and chemical analyses.

Radiocarbon dating was performed for one plant material using a standard accelerator mass spectrometer (AMS) method at the Beta Analytical Radiocarbon Dating Laboratory.

Volcanic ash was observed in detail under the microscope to determine the mineral composition, refractive index and morphology of the glass shards following the procedure adopted by Yoshikawa (1983). Then the volcanic ash layer was correlated with the

known marker tephra based on the microscopic features and stratigraphic position.

Dried sediment samples were ground with an agate bowl, and digested with dilute HCl (3%) for 24 hrs to remove inorganic carbon fraction (carbonates). Samples were then dried on hot plate at 110°C supplying distilled water 2-3 times to remove the remaining HCl. Following the treatment, C and N were measured using the dry combustion technique in a CHN corder (YANAKO MT-5, Yanagimoto Seisakusho Co., Inc.), and the content of TOC and TN were expressed in weight percentage of dry weight of the original sediments.

Sediment samples for diatom analysis were taken from 50 horizons along the long core at intervals of 2 to 5 cm to cover all degrees of variations in TOC contents in the cored sediments. Slides were prepared

following the procedure given by the Diatom Research Group for Nojiri-ko Excavation (1980).

Slides were examined mostly under the high magnification (40×10), but oil immersion technique (100×10) was also used to reveal the detail of small diatoms. The motive of diatom study was mainly to measure the abundance and to see its relationship with the TOC content. For this purpose, all diatom frustules in 100 sections (each 0.01815 mm^2) along 10 transects were counted in each slide for 1 mg dry sediments based on the dilution rate of the sediments. The counting error including the non homogeneity of diatom distribution and statistical error was estimated about $\pm 3\text{--}5\%$ through the multiple counting of the same slides. No attempts were made to determine the abundance of individual taxon except the predominant one because of difficulty of precise identification.

Mackereth piston core sampler may disturb the uppermost part of the cored sediment. Therefore, we sampled another 23 cm long core at the same time (Fig. 4, Site B), keeping the water-sediment interface intact using a gravity corer to complement the disturbed part. The same procedures as mentioned above were followed for the short core also.

Results

1. Surface sediment distribution

Sediments in the eastern and western peripheral zone, shallower than 15 m, are mostly gravel, gravely sand, and sand (Fig. 5), which form staircase-like bedforms as shown in Fig. 3. These coarser sediments are irregularly distributed and have been exposed to the land surface during winter and early spring due to water level lowering since 1954, and hence subject to erosion and washing. Lake bottom deeper than 15 m, both in the main and sub-basins, is mostly covered by clayey silt, which occupies about 75% of the bottom surface (Fig. 5). Silty clay, the finest sediment in the lake, is confined only in a small area at the northwest corner of the lake under 15–20 m water depth. Sandy silt is also distributed only in a small lobate area off Kakura, southeastern margin of the main basin. The distribution of grain-size therefore does not show gradual change from the coarse materials in peripheral zone to the finest sediment in the central part of the basin.

Contour values of the median grain-size decrease northwestward, abruptly from 4.5 to 6.5, and gradually from 6.5 to 7.5 phi (Fig. 5). The contour lines are open to northwest side, and the center of 7.5 phi line locates at much northwestern part of the basin plain. The median diameter reduces to 8 phi for the silty clay, which is distributed only in the northwestern corner of the lake, where the water depth is 15–20 m.

2. Lithology of the cored sediments

The long cored sediment is mainly composed of homogenous olive black (7.5Y 3/2) to black (5GY 2/1)

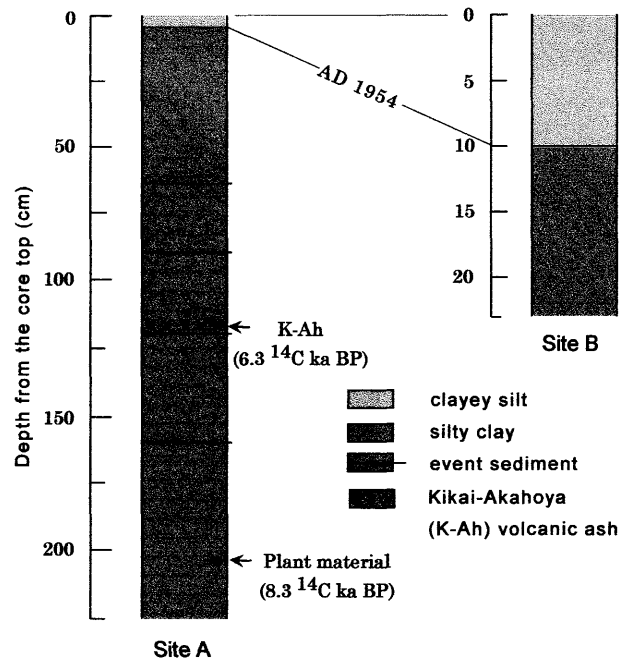


Fig. 6. Lithology of the cored sediments at Sites A and B in Lake Aoki. Age of the Kikai-Akahoya (K-Ah) volcanic ash and the plant material are shown.

AD 1954 is the starting of the Aoki hydropower generation.

silty clay except for the uppermost 5 cm, which is a little bit lighter in color and coarser in grain-size (Fig. 6). The lower boundary of the uppermost 5 cm is contorted due to the artificial disturbance of the sediments during sampling and recovery process. Coarse sand and granule grains are randomly scattered in the sediments as conformed by X-ray photograph. As in Lake Nakatsuna (Adhikari and Kumon, 2001), these scattered grains are interpreted as dropstones related with ice formation and drifting during winter and early spring.

Four light-gray layers of 3–5 mm thickness are intercalated at 65, 90, 125 and 158 cm. These layers are slightly coarser, sticky and very hard upon drying compared to the usual sediments. They display sharp lower boundary and contrasting diffuse upper boundary. Diatoms are much less in these layers than in the usual sediments. These features combined with higher proportion of coarser particles under smear slide observation suggest that they are flood-related event sediments. Sometimes terrestrial plant fragments were also observed in the coarser sediments.

The conventional age of the radiocarbon dated plant material at depth 206 cm is 8330 ± 40 yr BP, and is calibrated to 9400 cal BP according to INTCAL98 (Stuiver et al., 1998). A volcanic tephra layer is intercalated at 121–122 cm depth of the long core (Fig. 6, Site A). It has discrete boundaries, light brown color and sugary appearance. Grain size ranges from coarse silt to fine sand size, and the materials consist of three

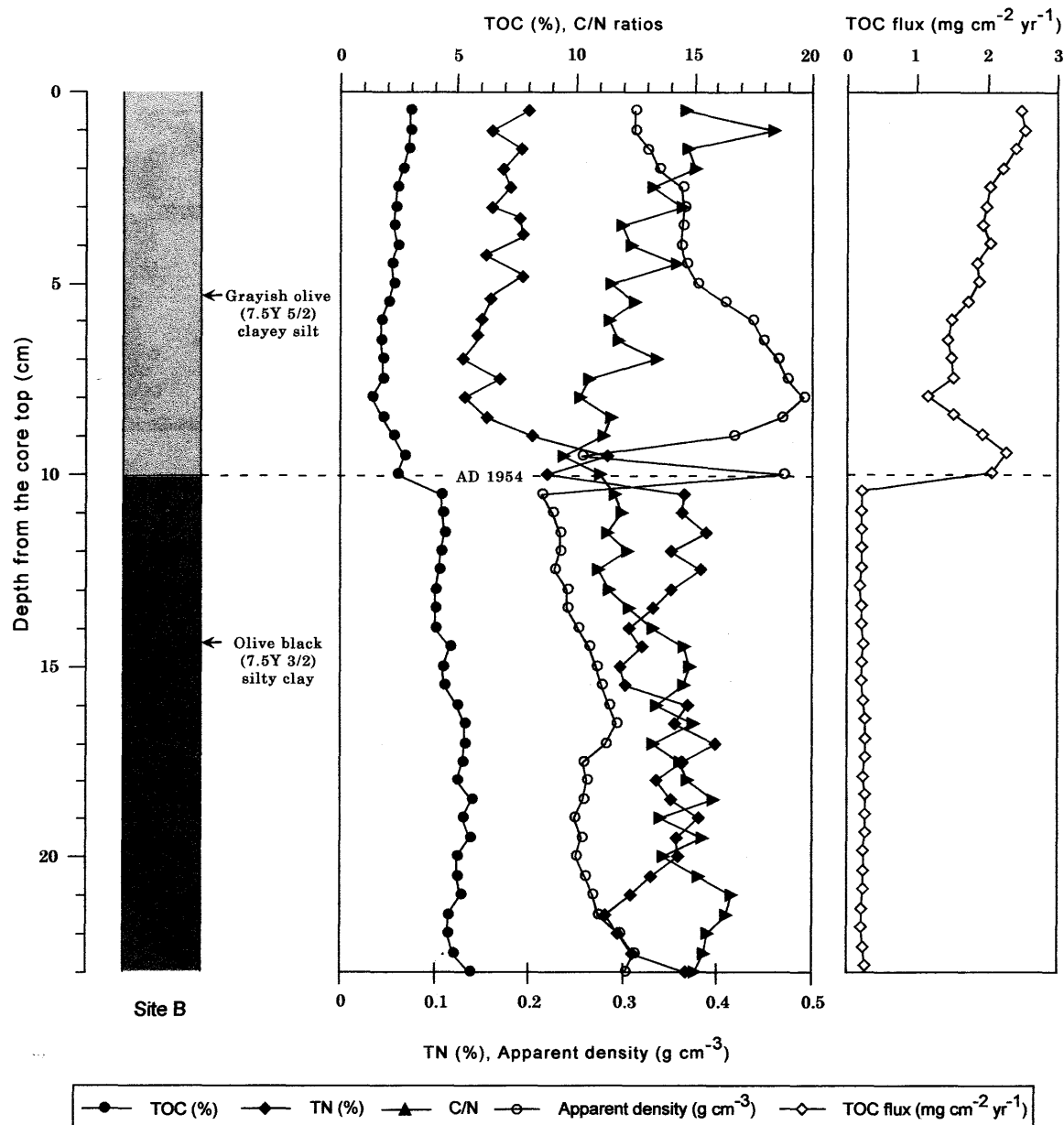


Fig. 7. Distribution of apparent density, total organic carbon (TOC) and total nitrogen (TN) contents, and C/N ratios in the 23 cm long sediments at Site B. TOC and TN are in weight percent, and C/N is their ratio. This surface core sample is undisturbed, keeping the water-sediment interface intact.

The sharp color contrast at 10 cm corresponds to the sharp break in apparent density, TOC and TN contents, and C/N ratios.

different types of glass shards, i.e., bubble-wall type (70%), plate glass type (25%) and fibrous type (5%) with refractive index in the range of 1.509-1.516. Heavy mineral phases are mainly ortho- and clinopyroxenes.

The short core is composed of grayish olive (7.5Y 5/2) clayey silt for the top 10 cm, and olive black silty clay (7.5Y 3/2) below that depth (Fig. 7). The upper part seems slightly coarser than the lower part. The boundary is horizontal and sharp, and corresponds with the abrupt change of apparent density and TOC content as shown in Fig. 7. The color contrast may be

due to these differences. The upper 10 cm sediments of this core correspond to the 5 cm of the long core (Fig. 6), which was disturbed in sampling process as mentioned before.

3. Water content and apparent density

Water content, a measure of the difference in the weight between freshly extruded samples before and after drying at 105°C for 12 hrs, gradually decreases downward from about 80% to 70%, but for the event sediments it is as low as 50% (Fig. 8). The water content abruptly decreases from 80% to 62% for the sediments above 5 cm depth. Apparent density was

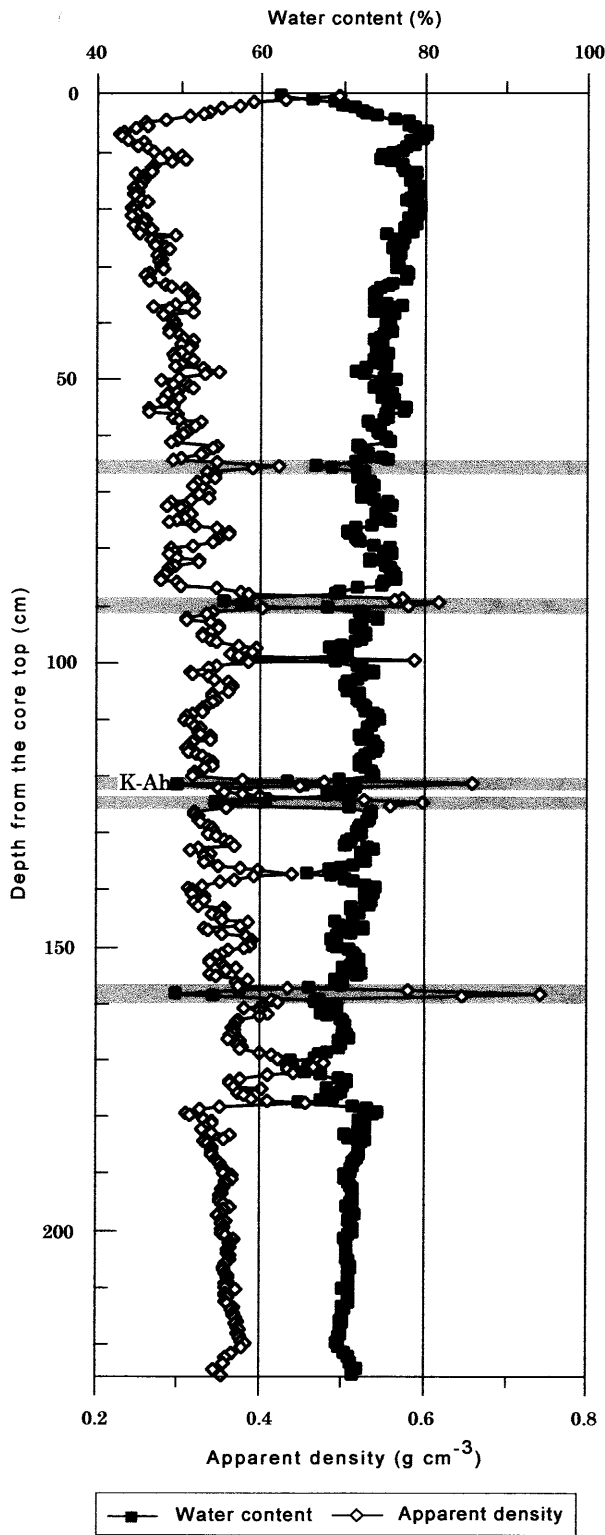


Fig. 8. Variation in water content and apparent density with depth in the cored sediments at Site A. Apparent density is solid weight per unit space calculated from dry weight and water content. *Shaded* parts indicate the event sediment intervals. K-Ah stands for the Kikai-Akahoya volcanic ash.

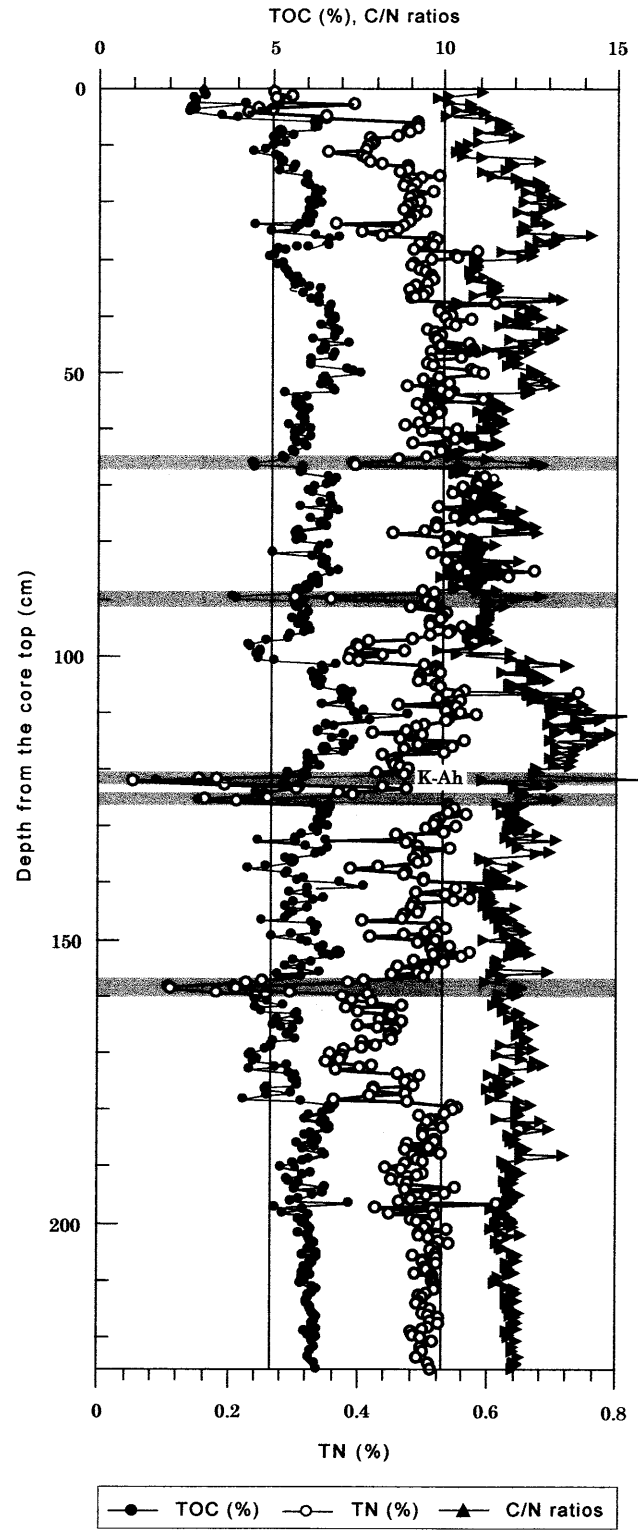


Fig. 9. Variation in TOC and TN contents and C/N ratios with depth in cored sediment at Site A. *Shaded* parts indicate the event sediment intervals. K-Ah stands for Kikai-Akahoya volcanic ash.

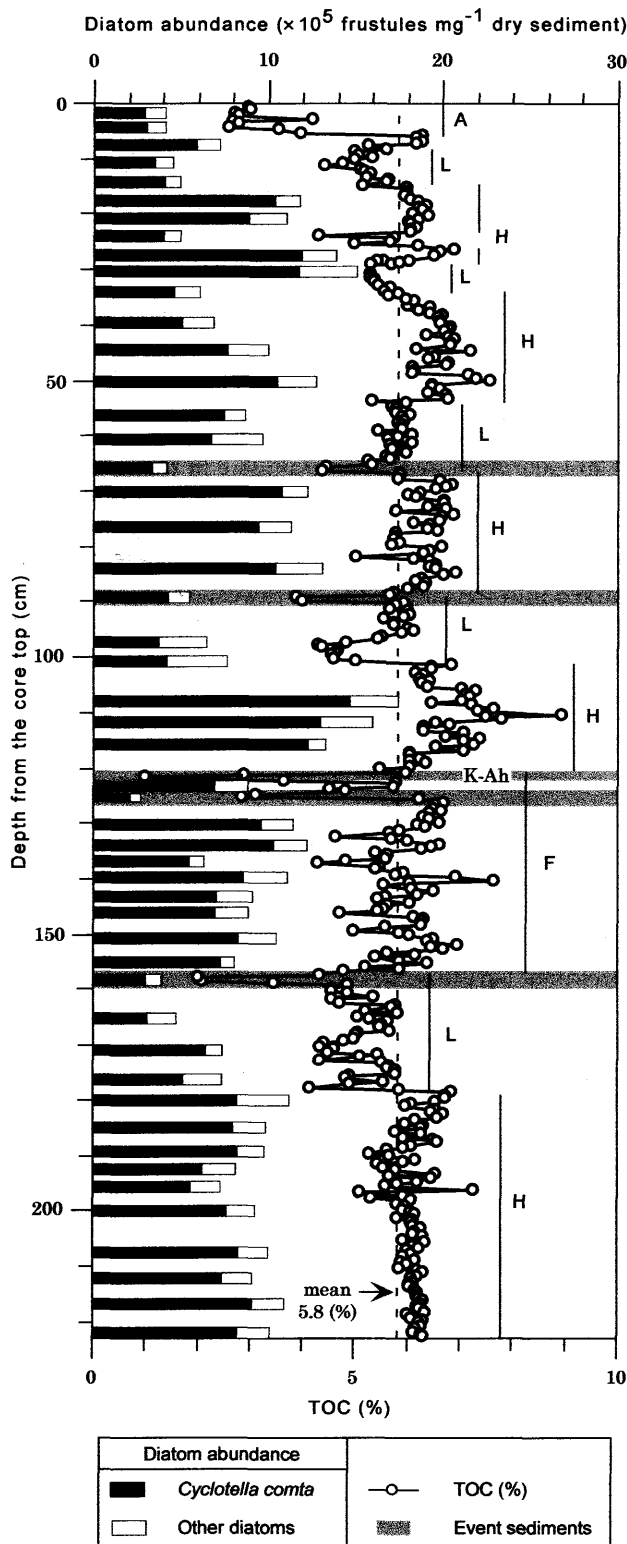


Fig. 10. Variation of diatom abundance with TOC contents in the cored sediments with depth at Site A.

Relative abundance of *Cyclotella comta* and other diatoms are also indicated. The letters H, L, and F are used to describe the variation in TOC content in relation to the mean value, where H-high (mostly above the mean), L-low (mostly below the mean), and F-fluctuating (fluctuating about the mean). A-indicates artificial influence after 1954.

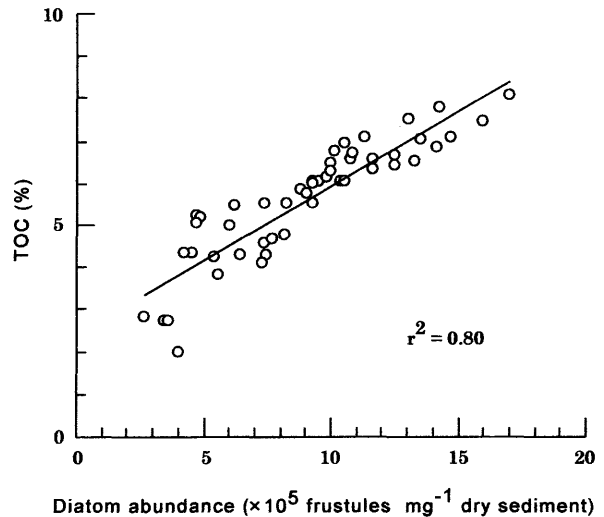


Fig. 11. Relationship between diatom abundance and TOC contents in the cored sediments at Site A.

calculated as solid weight per unit volume based on dry weight and water content, postulating grain density as 2.65 g/cm^3 . Generally, it fluctuates between 0.25 to 0.40 g/cm^3 , with a long-term trend gradually increasing downward with some exceptional sudden peaks at the volcanic ash horizon or at the event sediment intervals (Fig. 8). An unusual upward density increase occurs above 5 cm depth at Site A. This increase is due to the artificial compaction during sampling process, because the undisturbed sediment in the short core shows a gradual increase to 10 cm depth and followed by a sudden decline (Fig. 7).

4. TOC and TN contents

TOC content generally varies between 4 and 7%, fluctuating about the mean of 5.82% and 5.78% for 5–121 cm and 121–225 cm, respectively. The mean for the whole profile is thus 5.8%. TN content and C/N ratios vary from 0.30 to 0.55% and 10 to 14, respectively (Fig. 9). Besides these ranges, the contents of TOC of the samples from the volcanic ash and event sediments fall as low as 1%, due to the dilution effect caused by temporal mixing of inorganic or low-organic materials. TOC and TN profiles show concordant fluctuations both in short- and long-term. C/N ratios also display oscillations roughly parallel with TOC content, but the ratios elevate at the event sediment intervals (Fig. 9) due to higher contribution of terrestrial organic matter. As the TOC and TN have parallel increase or decrease at every level, TOC will be mentioned hereafter to represent the both.

The TOC record displays five intervals during which the TOC content is above the mean (high), five intervals in which the TOC is below the mean (low), and one interval for which the TOC values fluctuate about the mean (Fig. 10). They are quasi-periodic and show various degrees of short-term fluctuations within each interval. The intervals of high TOC con-

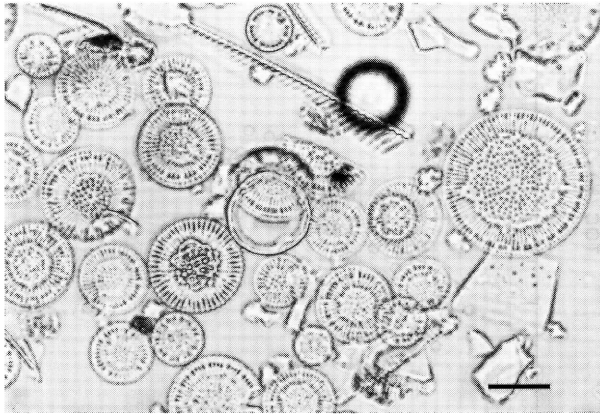


Fig. 12. Photomicrograph of the predominant diatom taxon, *Cyclotella comta*.

The scale bar at the right corner is 0.01 mm.

tent are evident at 17 to 27, 34 to 53, 67 to 89, 103 to 121, and 179 to 225 cm, although the first and the last intervals have some brief interruptions. TOC reaches to its highest level (8%) between 103 and 121 cm. Low values are prevailed between 5 and 17, 27 and 34, 53 and 67, 89 and 103, and 157 and 179 cm. The only interval with high magnitude fluctuation about the mean is between 121 and 157 cm. Following a brief highs between 5 and 7 cm, TOC contents above 5 cm abruptly decrease to the level of 2.5%, which is the lowest content in the cored sediment, except for the event sediments (Fig. 10). The artificial flow introduced into the lake since AD 1954 may have caused this low value.

5. Diatom abundance

Diatom number counted under 100 sections in a slide for the usual sediments varies from 406 to 1602 cells, which corresponds to 4.46×10^5 and 17.85×10^5 valves mg^{-1} dry sediment, respectively (Fig. 10). The least number is observed at 11 cm, while the abundance is peaked at 108 cm depth and decrease to a minimum of 2.24×10^5 valves mg^{-1} dry sediment at 125 cm depth. In the event sediments, the abundance is invariably lower than in the usual sediments. Two samples from the uppermost 5 cm have also lower diatom abundance than the lower limit in the usual sediments. A simple linear regression line shows a significantly positive correlation between diatom abundance and TOC concentration in the sediments ($r^2 = 0.8$) (Fig. 11).

The most common diatom is characterized by a circular valve face with a well-defined outer zone of radial alveoli and circular network of puncta in the central part (Fig. 12). These features suggest that it is *Cyclotella comta*, which occupies about 70–89% of the diatoms in all samples examined (Fig. 10), but no other *Cyclotella* taxa were observed. Abundance of total diatom and the number of *C. comta* have statistically significant positive correlation ($r^2 = 0.92$). The relative

abundance of the rest of the diatoms throughout the core therefore represents only about 11–30% of the flora in which the most common genera identified are *Aulacoseira*, *Navicula*, *Tabellaria*, *Cymbella*, *Pinnularia*, *Diploneis*, *Fragilaria*, *Synedra*, *Eunotia* and *Gomphonema* roughly in an order of decreasing abundance. *Synedra* and *Tabellaria* are completely absent in some slides observed, such as at 177.5 and 179.5 cm. Broken fragments of *Fragillaria*, *Synedra* and *Tabellaria* are evident at several levels most probably due to the heating effects during slide preparation.

Discussion

1. Modern hydraulic conditions

In Lake Aoki, sediment grain-size in the inner zone decreases northwestward as described before (Fig. 5). It is quite unusual, but evident that the observed distribution is largely influenced by the artificial flow mixed into the lake at the southwestern margin since 1954. The artificial inflow ($2.69 \text{ m}^{-3} \text{ s}^{-1}$) for the use of electric power generation is as much as 4.6 times of the total natural inflow ($0.58 \text{ m}^{-3} \text{ s}^{-1}$) from its natural catchment (Watanabe et al., 1987). Moreover, snow-melt water is abundantly added into the lake in spring to recover the lowered water level in winter, which contains a lot of silt and clay materials. These materials are transported northwestward, settling particle en routes according to its grain-size. Therefore, higher proportion of clay deposits in the remote northwest corner, leaving the coarser fraction in the proximal part (Fig. 5).

Besides the change in sediment grain-size, the hydraulic change also results in the difference of density, color, and TOC content between the upper and lower part of the short core (Fig. 7). The clayey silt (upper 10 cm) is of high density, and has light color compared with the lower part, corresponding to the low carbon content. The reason of higher density is considered that the artificial flow has supplied coarser sediment into the lake since 1954, especially in early spring. Considering the boundary of 10 cm depth is AD 1954, the sedimentation rate reaches at 2.22 mm yr^{-1} ($85 \text{ mg cm}^{-2} \text{ yr}^{-1}$). This rate is much larger than the sedimentation rate below it ($0.16 \text{ mm yr}^{-1}/5 \text{ mg cm}^{-2} \text{ yr}^{-1}$, see chronology section). This difference also can be explained by the mixing of the artificial inflow as mentioned above. Before this modification, the grain-size of the sediment was much finer, and calm condition prevailed with a little water inflow.

The TOC content in the upper 10 cm of the short core appears low (Fig. 7), but this low content is mainly due to the dilution effect caused by the abundant supply of inorganic materials. The TOC flux, the TOC amount accumulated per unit area per unit time, is much higher than the lower part. This abrupt increase is attributed to the supply of larger amount of nitrogen (N) and phosphorous (P) into the lake

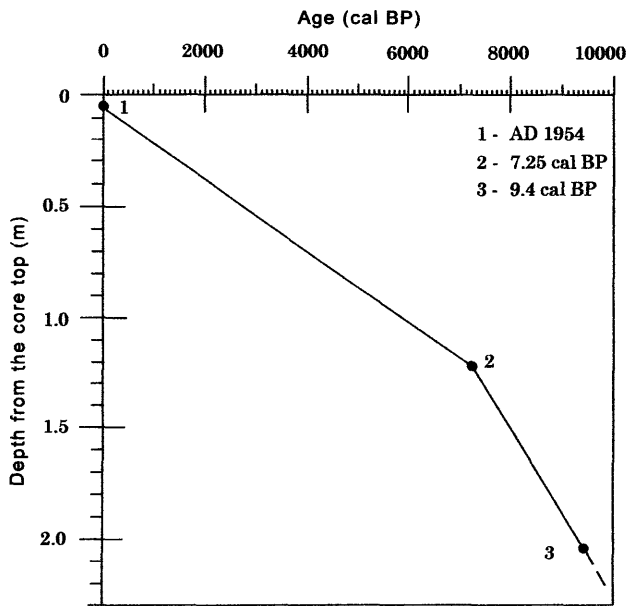


Fig. 13. Depth-age relationship of the cored sediments at Site A.

Dashed part of the line indicates extrapolation of the reference ages.

following the introduction of the artificial flow, which is 3 to 4 times higher than that before 1954 (Omachi City Office, 1983). The artificial inflow adds nutrient continuously to the lake water, and induces vertical water circulation in part as well. These conditions have been supporting large biological productivity compared to that of the lower part.

2. Chronology and sedimentation

The volcanic ash at 121–122 cm in the long core is correlated with the well-known widespread tephra, Kikai-Akahoya (K-Ah) erupted from the Kikai Caldera, south Kyushu. Many researchers have measured the age of K-Ah, and the mode of the measured ages lies at 6300 yr BP (Machida and Arai, 1983). The radiocarbon dating of the plant material at 206 cm depth yields a conventional age of 8330 ± 40 yr BP. According to INTCAL98 (Stuiver et al., 1998), these two ages are calibrated to 7250 and 9400 cal BP, respectively. Recently, Kitagawa et al. (1995) measured the K-Ah tephra age as 7286 cal BP, based on varve counting and ^{14}C dating. As discussed above, the 5 cm depth in the long core corresponding to the 10 cm depth in the short core is considered to be AD 1954. These three reference ages, AD 1954, and 7250 and 9400 cal BP, are used here as the controlling points to estimate sediment age as shown in Fig. 13.

The average sedimentation rate and age of sample horizons were derived by interpolating these reference ages above 206 cm depth and extrapolating below that depth, supposing that sedimentation rate is constant for each interval (Fig. 13). The average sedimentation rates of 0.16 mm yr^{-1} ($5 \text{ mg cm}^{-2} \text{ yr}^{-1}$)

between 5 and 121 cm and 0.37 mm yr^{-1} ($12.25 \text{ mg cm}^{-2} \text{ yr}^{-1}$) between 122 and 225 cm and their sampling interval of 0.5 cm has provided a temporal resolution of ca. 29 and 13 years, respectively.

The change in the sedimentation rate is explained by comparing the two sediment cores each drilled from the main-and sub-basins (Inouchi et al., 1987). The uppermost part of the cored sediments from the sub-basin (close to our Site A) is much shorter than the correlative upper part of the cored sediments at the deep main basin, indicating much reduction in sedimentation rate around our sampling sites. The difference is explained by the bathymetric change induced by an active fault with dip slip geometry running along the cliff that separates the northeastern sub-basin and main basin (Fig. 4) (Kumon and Inouchi, in press). This fault is a branch of the Itoigawa-Shizuoka Tectonic Line, and its intermittent activity made the main basin low, forming distinct topographic difference. The terrigenous lake has the tendency that sediment is focused in the deeper part of the basin (Inouchi et al., 1987). Therefore, sedimentation rate has reduced in the sub-basin following the growth of the fault cliff.

3. Implications of TOC, TN, C/N ratios and diatom

Organic matter in lake sediments may be derived from lake planktons and terrestrial plants. Generally, nonvascular aquatic plants have C/N ratios less than 8 whereas vascular land plants, which contain cellulose, have C/N ratios above 30 (Nakai and Koyama, 1987). The range of C/N ratios, i.e., 10–14, in Lake Aoki sediments therefore suggests that lake plankton are the major source of the organic matters in the sediments in association with minor land plants.

Theoretically, it is reasonable to suppose that biogenic productivity in lake water affects the amount of organic residue in the sediment through food-chain and decomposition process, so that high productivity corresponds to high flux of organic material in sediments. The organic flux in the sediments is proportional to the TOC and TN contents under the condition of constant sedimentation rate. The concordance of diatom abundance and TOC contents as shown in Fig. 10 supports this idea.

The biogenic productivity is affected by nutrients and water circulation. As discussed in the section of modern hydraulic condition, the biogenic productivity is much increased by abundant N and P supply due to the artificial inflow mixing since 1954. Another important factor that controls lake productivity is water temperature. High water temperature makes living things more active and enhances biogenic productivity except for extremely high temperatures. The average temperature of surface water in Lake Aoki is 9.4°C , and lake surface sometimes undergoes freezing in part in winter. Water temperature is con-

trolled directly by the atmospheric temperature. Therefore, warm climate may induce high biogenic productivity, resulting in high organic flux in the lake sediment. For example, the productivity of Lake Suwa, as measured by chlorophyll *a* showed a distinct reduction in 1993 with cool summers, and indicated much increasing in 1994 with hot summer (Park et al., 1998).

Some studies have also shown that warm condition appears to have an important effect on the relative abundance of diatom and other freshwater algae (e.g., Stoermer and Ladewski, 1976; Tilman and Kiesling, 1984; Xiao et al., 1997). The low and high contents of TOC and TN which correspond to the Little Ice age (LIA) and the Medieval Warm period (MWP), respectively, were reported in Lake Nakatsuna (Adhikari and Kumon, 2001) and Lake Kizaki (Kumon, 2001). Similarly, pollen analysis also clarified correspondence of warm climate with high TOC and TN contents (Kumon et al., 2000). Inouchi et al. (1996) also reports that TOC in the sediments of Lake Biwa fluctuates well, corresponding with cold-warm cycles such as glacial-interglacial intervals.

The sediment before 1954 shows no distinct difference in grain-size except for event sediments mentioned before, suggesting no significant change in hydraulic condition of the lake. Diatom composition characterized by the predominance of *Cyclotella comta* also implies that oligotrophic condition have been continued. Therefore, we conclude that the fluctuation of TOC and TN contents can be regarded as a proxy of temperature variability, if the sedimentation rate is constant.

Although the sedimentation rate can be decreased gradually upward, it is difficult to know precisely with the available data. We therefore consider constant rate above and below 7250 cal BP, separately. As the comparison between the two segments has no meaning, the relative abundance of TOC and diatom can be correlated with the warm-cool fluctuations within each interval.

When the carbon flux is calculated on the basis of carbon content and sedimentation rate, large difference exists in carbon flux between the two intervals. This difference also relates to the cause that changes the sedimentation rate itself by forming high relief of the cliff between the sub-basin and main basin. In the similar process, organic matters tend to move with fine particles such as clay, resulting in the concentration in the deeper part of the basin. This example is shown in the work of Lake Nakatsuna (Adhikari and Kumon, 2001). The concentration decreases at the shallower part of the basin just as the upper part of the cored sediment at Site A.

4. Climatic reconstruction of the Holocene

Discounting the short-term century scale oscillations superimposed on the long-term decreasing and

increasing trends, the observed high, low, and fluctuating TOC contents, and diatom abundance are grouped into 11 qualitative phases broadly typified by warm, cool and fluctuating climates, respectively (Fig. 14). We consider that the large positive and negative deviations of the TOC contents from their mean roughly indicate the degree of warmness and coolness, respectively, within the period of the same sedimentation rate. Among the reconstructed phases, five warm periods span between ca. 750–1300, 1750–3050, 4000–5250, 6150–7250, and 8800–10000 cal BP; five cool periods are evident during 150–750, 1300–1750, 3050–4000, 5250–6150, and 8350–8800 cal BP, and the remaining one period occurring at 7250–8350 cal BP is characterized by fluctuating climate. Notably, almost every climate phase has abrupt onset and termination throughout the record. All the climate phases are grouped into two parts as separated by the K-Ah horizon based on the difference in the sedimentation rate, and the individual phase is described below starting from the younger age.

(1) Present to middle Holocene (Present to 7250 cal BP ; 0–121 cm) : Since the sediment after AD 1954 is artificially influenced, it is excluded from the climatic discussion below. A century long warm condition prevails between AD 1950–1850, which can be interpreted as the reflection of the modern warming (MW) (Fig. 14).

First cool phase-HC1 (AD 1250–1850 ; 17–5 cm) : The four centuries between AD 1250–1850 are the latest cool phase with various degrees of cooling culminating around AD 1550 (Fig. 14). Sakaguchi (1983, 1993) recognized the cooling after AD 1300 as the Little Ice Age (LIA) in Japan. Historically, the LIA in Japan is often correlated to the Edo Period (AD 1603–1868), during which three big famines occurred (Fukuoka, 1992; Sugihara and Yamanaka, 1992). From the neighboring Lake Nakatsuna, Adhikari and Kumon (2001) reported cool phase from AD 1200 to 1950, in which the greater cooling from AD 1300 to 1470, 1700 to 1760, and 1850 to 1950 are interpreted as the LIA cool phases. The cool phase we noted here between AD 1250–1850 is correlated with the LIA, but in contrary to others, it appears as a sustained cool phase although the magnitude of cooling is variable.

There is a general agreement that glaciers around the world expanded during at least part of the 13th to 19th centuries (Grove, 1988), a period called the LIA. This cool event is also recognized in the paleoclimate records from Europe, North America, and the southern Hemisphere (Harvey and Schneider, 1985). Regarding the magnitude of cooling, it has been estimated that LIA was about 1–1.5°C cooler in reference to the present day temperature (Bernabo, 1981; Rind and Overpeck, 1993).

First warm phase-HW1 (AD 700–1250 ; 27–17 cm) : The phase encompassing AD 750–1250 is warm with a brief

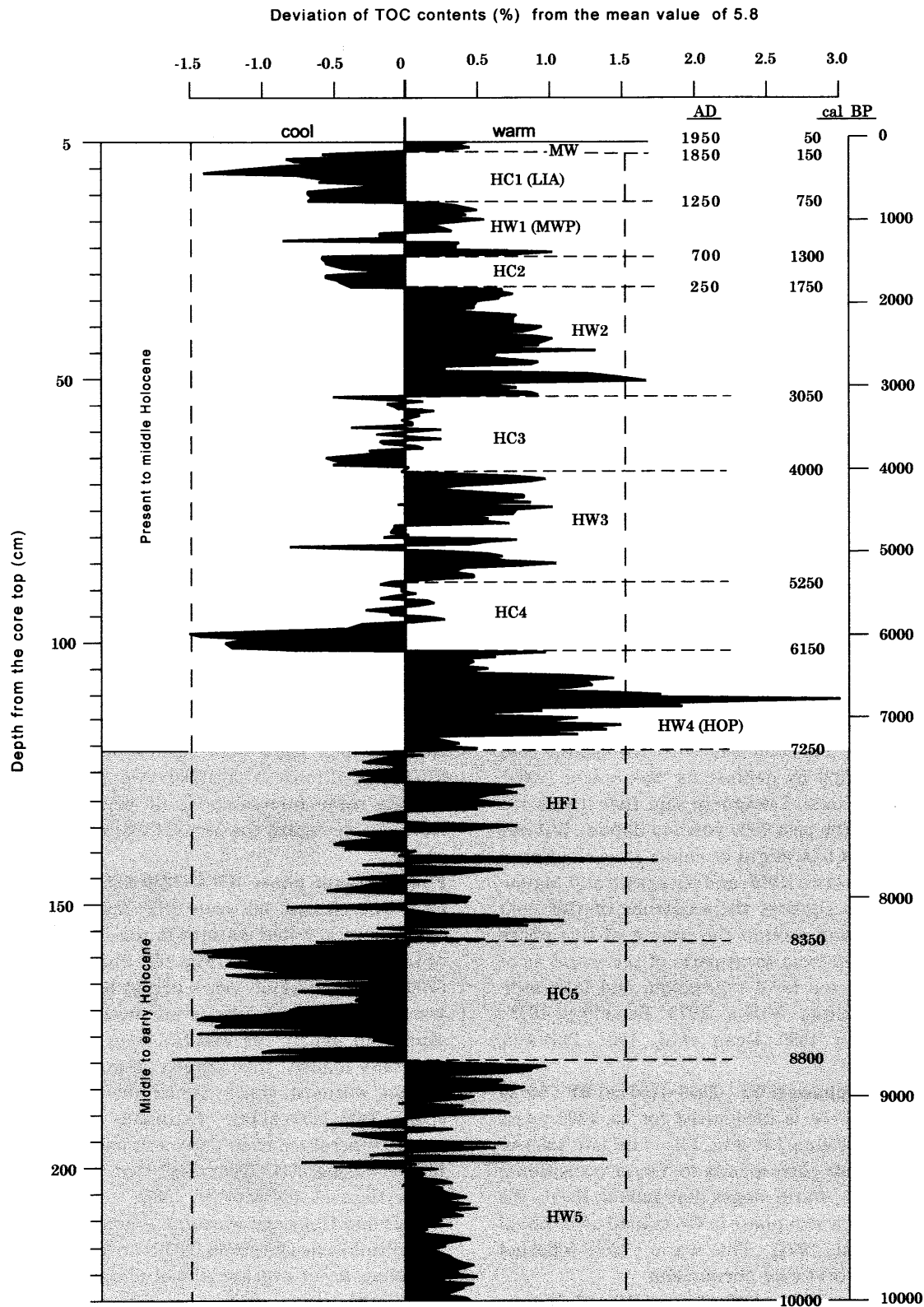


Fig. 14. Reconstructed climate variability during the Holocene period based on the deviation of TOC contents from their mean value of 5.8%.

Event sediment intervals are excluded. Ages are based on the depth-age relationship as shown in Fig. 13. Age calibration is based on Stuiver et al. (1998). As the shaded part below has higher sedimentation rate than the overlying part, magnitude of climate cooling and warming between these two parts can not be compared. Climate phase boundaries are placed where the deviations of TOC contents show remarkable changes. The abbreviations are as follow : MW-the modern warming, HC1-5-Holocene cold phases, HW1-5-Holocene warm phases, HF1-Holocene fluctuating phase, LIA-the Little Ice Age, MWP-the Medieval Warm Period, and HOP-the Holocene Optimum.

but pronounced cool episode centered around AD 900 (Fig. 14). In Japan, the period AD 732–1296 is called the 'Nara-Heian-Kamakura warm stage', during which the sea level was a little higher than today (Sakaguchi, 1983). There is a well-supported evidence from $\delta^{13}\text{C}$ record of tree rings (Kitagawa and Matsumoto, 1995) from Japan that the period between AD 700–1300 was warm. Other lake sediment based reconstruction from Japan (e.g., Inouchi et al., 1996, Fukusawa, 1996; Kumon, 2001; Adhikari and Kumon, 2001) also report the existence of the MWP in central Japan.

The warm period spanning AD 800–1300 was originally reported from western Europe and known as the Medieval Warm Period (MWP) (e.g., Hughes and Diaz, 1994). A continuous warm phase is also apparent for AD 650–1200 in the GISP2 core record from central Greenland (Meese et al., 1994).

The warm phases between AD 650–1350 are known by the 'Pulandian warm period' in China (Duan et al., 1981). It is divided into two warm phases, AD 950–1350 and 650–750, by a cold episode. Similarly, Stine (1994) reports the MWP in California in two phases, AD 892–1112 and 1209–1350. We also interpret the warm phase between AD 700–1250 in our record as the indicative of the MWP occurring in two phases separated by a cool spell (Fig. 14).

Second cool phase-HC2 (AD 250–700; 34–27 cm): Before the MWP, the climatic deterioration between AD 250–700 (Fig. 14) coincides with the Kofun cold stage (AD 240–732) as defined by Sakaguchi (1983). Based on pollen data, Sakaguchi said that it was the coldest stage in the past 7600 years in Japan. But our data suggest that LIA might be colder than the Kofun cold stage. Fukusawa (1996) and Kitagawa and Matsumoto (1995) also support the existence of this cold stage. The cooling around the timing of this phase has been reported from most parts of the world as of glacial advance, sea level regression, and lake sediments records (e.g., Miller, 1973; Benedict, 1973; Nakai and Hong, 1980; Duan et al., 1981; Bernabo, 1981; Chinn, 1981).

Second warm phase-HW2 (3050–1750 cal BP; 53–34 cm): A warm phase is recognized for ca. 1300 years spanning 1750–3050 cal BP (Fig. 14). The late part of this climate phase corresponds to Yayoi transitional and Jomon-Yayoi warm stages (Sakaguchi, 1993). We can find a coeval warm phase in Greenland after 2.8 cal ka BP (Bond et al., 1997). This warm phase reported here might be worldwide phenomena.

Third cool phase-HC3 (4000–3050 cal BP; 67–53 cm): Starting with a cool environment, the middle and late parts of 3050–4000 cal BP are intercalated with five minor decadal to century scale warm spells, which collectively we designate as the cool phase (Fig. 14). During a part of this period, sea level regression was recognized and correlated with the cold climatic condition in Japan (Umitsu, 1976; Hirai, 1983). This cool

phase partly coincides with the Latest Jomon cold stage and Jomon transitional stage in Japan (Sakaguchi, 1983, 1993). For the first half of this phase, Anderson et al. (1998) has reported evidence of abrupt climatic change in northern Scotland. Bond et al. (1997) also points that there existed a cool episode in northern Atlantic region around 3.2 cal ka BP.

Third warm phase-HW3 (5250–4000 cal yr BP; 89–67 cm): Although punctuated by three brief cool episodes at around the middle part, a warm phase is recognized during ca. 5250–4000 cal BP (Fig. 14). It almost corresponds to the the First and Second late Jomon warm stages (Sakaguchi, 1983) and Middle Jomon minor transgression in Japan (Ota et al., 1982). According to them, high sea levels were often recognized not only in Japan, but also throughout the world. Similar warming was experienced at least during a part of this period in Iceland and California (La Marche, 1973) and South Korea (Nakai and Hong, 1980).

Fourth cool phase-HC4 (6150–5250 cal BP, 103–89 cm): Climate shifts to entirely opposite mode between 6150–5250 cal BP. Temperature drops sharply down to the lowest level for the early half and the magnitude of cooling decreases for the second half with the intercalation of two subordinate warm events (Fig. 14). The timing of this cooling partly coincides with the microfossil records from Pacific Ocean and south Korea, which show cool episode between 4500 and 5700 cal BP (Chinzei et al., 1980; Nakai and Hong, 1980). Despite some intercalations of warm episodes, collectively we regard the period 6150–5250 cal BP as cool phase.

Fourth warm phase-HW4 (7250–6150 cal BP; 121–103 cm): The climate between 6150–7250 cal BP switches over unprecedented warmth in the 7250 years history of Lake Aoki sediments (Fig. 14). Culminating around 6700 cal BP, this 1100 years period is the persistently warm phase bounded by pronounced drop in temperature. In Japan, the mid-Holocene transgression is generally called the 'Jomon transgression'. The Jomon warmest stage named by Sakaguchi (1983) spans 5300–7250 cal BP. Estimates of mean annual paleotemperature from Japanese pollen data is $\sim 2^\circ\text{C}$ higher during 6000–7000 cal BP than present temperatures (Heusser and Morley, 1985).

This mid-Holocene warming is generally referred to as the Holocene Optimum (HOP) or Altithermal, corresponding to an average global temperature of about 2°C higher than nowadays (e.g., Petit-Maire and Bogsse, 2000). Loess, paleosol, and glacier studies in Tibet and Western China also suggest prevalence of warmer and wetter condition in middle Holocene than today (Wang and Fan, 1987; Fang, 1991; Zhou et al., 1991). Evidences from other sources also indicate the maximum Holocene warmth between 6000 and 8000 cal BP (Heaton et al., 1986; Talma and Vogel, 1992)

with a warming of ca. 1–2°C with respect to the present day situation. The warming between 7250–6150 cal BP reported here is considered to be the HOP, because it is quite close to the timing of the HOP reported in the literatures as mentioned above.

(2) Middle to early Holocene (7250–10000 cal BP ; 121–225 cm) : This period has 3 phases ; each represents warm, cool, and fluctuating climate. As the sedimentation rate during this period is more than two times higher than that after it, the TOC flux converted from the TOC contents is much different from the later one. As discussed before, the change in sedimentation rate is due to the fault activity along the basins' divide. Because of this reason, the magnitude of climate warming or cooling can not be compared with those after 7250 cal BP.

Fluctuating climate phase-HF1 (8350–7250 cal BP ; 156–121 cm) : Before the HOP, a new scenario characterized by a series of warm and cool episodes each lasting about a century or more appears roughly in a semi-periodic fashion for about 1100 years between 7250–8350 cal BP (Fig. 14). We refer this combination as the fluctuating climate. Such type of climatic fluctuation may be related with transitory changes in climate system (O'Brien et al., 1995). This fluctuating climate phase partly corresponds to the Early Jomon warmest stage in Sakaguchi's reconstruction (1983).

Fifth cool phase-HC5 (8800–8350 cal BP ; 180–156 cm) : Cooling occurs for ca. 450 years spanning 8800–8350 cal BP (Fig. 14). From the Greenland ice-core proxies, Alley et al. (1997) reports a prominent cooling event between ca. 8400–8000 cal BP, which was approximately half the magnitude of Younger Drays. The duration and magnitude of cooling of this phase is correlative with the ice-core record, but the timing is about 400 years earlier. This may be due to geographical leading.

Fifth warm phase-HW5 (10000–8800 cal BP ; 225–180 cm) : Although there exist some fluctuations after the central part, the interval spanning 10000–8800 cal BP is considered as a warm phase (Fig. 14). It is a long warm phase of a smaller magnitude, and seems to be the first warm phase of Holocene time. Similar warm phase is often reported between the Younger Drays and the Boreal Period also.

Conclusions

The modern hydraulic changes in the lake after 1954 have significantly influenced sediment grain-size distribution, sedimentation rate and carbon flux in the sediment. The dropstones related with ice bounding and drifting on the lake surface are randomly scattered in the sediments. Both long- and short-term fluctuations are evident in TOC content and diatom abundance and a close correspondence is existed between them. The diatom composition suggests that the lake has been oligotrophic and alkaline, and there

has been no evidence of lake eutrophification. Temperature appears to control TOC content and diatom abundance and serve as excellent climate proxy indicators.

The Holocene period is appeared to have significant climatic diversity with frequent shifting between warm and cool conditions in centennial to millennial scale. Five warm, five cool, and one fluctuating climate phases are recognized. Most of the warm phases are warmer than the present time. Notably, every climate phase has abrupt onset and termination. The most recent cold and warm phases well correspond to the LIA and MWP, and the warmest phase, the HOP is evident between 6150 and 7250 cal BP. Although the local temperature variability may obliterate the regional signature, the remarkable similarities of our reconstruction with the global climate fluctuations after 7250 cal BP suggest that the climate in the studied area was dynamic and sensitive to global climate forcing.

Acknowledgements

We thank K. Kanamaru, S. Naganuma, O. Ken, K. Fukushima, M. Kasuga, B.K. Adhikari, and T. Honma for their assistance in the field sampling and laboratory analysis. We are grateful to Prof. T. Murakami for his guidance that improved our diatom taxonomy and Y. Takeshita for his help in the determination of refractive index of the volcanic glass. Thanks are also due to Prof. Y. Inouchi, Prof. H. Hayashi, and M. Yamamoto for their helps in various ways. Special thanks go to Dr. K. Kashima and the second, anonymous reviewer who offered suggestions that greatly improved our manuscript.

References

- Adhikari, D.P. and Kumon, F., 2001, Climatic changes during the past 1300 years as deduced from the sediments of Lake Nakatsuna, central Japan. *Limnology*, **2**, 157–168.
- Alley, R.B., Mayewski, P.A., Sowers, T., Stuiver, M., Taylor, K.C. and Clark, P.U., 1997, Holocene climatic instability : a prominent, widespread event 8200 yr ago. *Geology*, **25**, 483–486.
- Anderson, D.E., Binney, H.A. and Smith, M.A., 1998, Evidence for abrupt climatic change in northern Scotland between 3900 and 3500 calendar years BP. *The Holocene*, **8**, 97–103.
- Benedict, J.B., 1973, Chronology of cirque glaciation, Colorado Front Range. *Quatern. Res.*, **3**, 584–599.
- Bernabo, J.C., 1981, Quantitative estimates of temperature changes over the last 2700 years in Michigan based on pollen data. *Quatern. Res.*, **15**, 143–159.
- Bond, G., Showers, W., Cheseby, M., Lotti, R., Almasi, P., deMenocal, P., priore, P., Cullen, H., Hajdas, I. and Bonami, G., 1997, A pervasive millennial-scale cycle in North Atlantic Holocene and glacial climates. *Science*, **267**, 1005–1010.
- Chinn, T.J.H., 1981, Use of rock weathering-rind thickness for Holocene absolute dating in New Zealand. *Arc. Alp. Res.*, **13**, 33–45.
- Chinzei, K., Oba, T., Koike, Y., Matsushima, Y. and Kitazato, H., 1980, Changes in oxygen isotope ratios of the shells

- from shell mounds and paleoenvironments in the prehistoric age. *Researches on archeological sites, cultural properties and so on by natural scientific methods*, 103–117.
- Diatom Research Group for Nojiri-ko Excavation, 1980, Diatom thanatocoenoses from the Nojiri-ko Formation. *Mem. Geol. Soc. Japan*, no 19, 75–100.**
- Duan, W., Qingyu, P. and Xihao, W., 1981, A preliminary study of Quaternary climatic changes in China. In Central Meteorological Agency, ed., *Selected papers of the conference 1978 on climatic changes in China, Beijing*, 7–17.
- Fang, J. Q., 1991, Lake evolution during the past 30,000 years in China, and its implication for the environmental change. *Quatern. Res.*, **36**, 1–24.
- Fukuoka, Y., 1992, The dendroclimatological study on the Little Ice Age in Japan. In T. Mikami, ed., *Proc. Intern. Symp. on Little Ice Age Climate*, 71–74.
- Fukusawa, H., 1996, High-resolution reconstruction of environmental changes from the last 2000 years varved sediments in Lake Suigetsu, central Japan. In Mikami, T., Matsumoto, E., Ohta, S. and Sweda, T., eds., *Proc. 1995 Nagoya IGBP-PAGES/PEP-II Symp.*, 84–89.
- Geographical Survey Institute of Japan, 1999, Active fault map in urban area, Omachi, 1 : 25000, D. 1–368.**
- Grove, J. M., 1988, *The little Ice Age*. Methuen, London, 498 p.
- Harvey, L. D. and Schneider, S. H., 1985, Transient climate response to external climate forcing on 10^2 – 10^4 year time scale, Part 1 : experiments with globally averaged, coupled atmosphere and ocean energy balance model. *Journ. Geophys. Res.*, **90D**, 2190–2205.
- Heaton, T. H. E., Talma, A. S. and Vogel, J. C., 1986, Dissolved gas paleotemperatures and $\delta^{18}\text{O}$ variations derived from groundwater near Uitenhage, South Africa. *Quatern. Res.*, **25**, 79–88.
- Heusser, L. E. and Morley, J. J., 1985, Pollen and radiolarian records from deep-sea core RC14–103 : Climatic reconstruction of northeast Japan and northwest Pacific for the last 90,000 years. *Quatern. Res.*, **24**, 60–72.
- Hirai, Y., 1983, Lacustrine and sublacustrine microforms of Lake Ogawara with relation to the lake-level changes after the maximum postglacial transgression. *Ann. Tohoku Geogr. Assoc.*, **35**, 81–91.
- Horie, S., 1962, Morphometric features and the classification of all the lakes in Japan. *Mem. Col. Sci. Kyoto Univ., Ser. B*, **24**, Article 2 Biol, 191–262.
- Hughes, M. K. and Diaz, H. F., 1994, Was there a 'Medieval Warm Period', and if so where and when? *Climate Change*, **26**, 109–142.
- Inouchi, Y., 1987, Acoustic estimation method of sedimentation rate - case study in Lake Biwa. *Chikyu Kagaku (Earth Science)*, **41**, 231–241.**
- Inouchi, Y., Yamazaki, H. and Shimokawa, K., 1987, Acoustic survey of Lake Aoki, Nagano Prefecture—a preliminary result. *Annual Meeting of Assoc. Quatern. Res. Japan*, no 17, 116–117.*
- Inouchi, Y., Yokota, S. and Terashima, S., 1996, Climatic changes around Lake Biwa during the past 300000 years and 2000 years. In Mikami, T., Matsumoto, E., Ohta, S. and Sweda, T., eds., *Proc. 1995 Nagoya IGBP-PAGES/PEP-II Symp.*, 109–114.
- Kawajiri, K. and Kumon, F., 1988, Surficial sediments of Lake Aoki in Nagano Prefecture, central Japan. *Clastic Sediments (Jour. Res. Gr. Clas. Sed. Japan)*, no 5, 85–94.**
- Kitagawa, H. and Matsumoto, E., 1995, Climatic implications of $\delta^{13}\text{C}$ variations in a Japanese cedar (*Cryptomeria japonica*) during the last two millennia. *Geophys. Res. Lett.*, **22**, 2155–2158.
- Kitagawa, H., Fukusawa, H., Nakamura, T., Okamura, M., Takemura, K., Hayashida, A. and Yasuda, Y., 1995, AMS ¹⁴C dating of varved sediments from Lake Suigetsu, central Japan and atmospheric ¹⁴C change during the late Pleistocene. *Radiocarbon*, **37**, 371–378.
- Kumon, F., 2001, Paleolimnological studies. In Saijo, Y. and Hayashi, H., eds., *Lake Kizaki*, Backhuys Publishers, Leiden, The Netherlands, 55–62 p.
- Kumon, F. and Inouchi, Y., 2002, Activity history of the Itoigawa-Shizuoka Tectonic Line along the Nishina-Sanko in central Japan, viewed from Lake Topography and sediments. In Tsukahara, H., ed., *Earthquakes and Protections in Relation to Itoigawa-Shizuoka Tectonic Line*, Shinanomachi Shinbunsha, 89–106.*
- Kumon, F., Kamitani, T., Sutoh, K. and Inouchi, Y., 1993, Grain size distribution of the surface sediments in Lake Biwa, Japan. *Mem. Geol. Soc. Japan*, no. 39, 53–60.**
- Kumon, F., Ohno, R., Sakai, T., Sakami, S. and Sakai, J., 2000, Climatic records during the last 40000 years in Lake Nojiri, central Japan. In Mikami, T., ed., *Proc. Int. Conf. Climate Change and Variability*, 41–44.
- LaMarche, Jr. V. C., 1973, Holocene climatic variations inferred from treeline fluctuations in the White Mountains, California. *Quatern. Res.*, **3**, 632–660.
- Machida, H. and Arai, F., 1983, The very widespread tephra—The Aira TN ash. *Kagaku (Science)*, **46**, 339–347.
- Meese, D. A., Gow, A. J., Grootes, P., Mayewski, P. A., Ram, M., Stuiver, M., Taylor, K. C., Waddington, E. D. and Zielinski, G., 1994, The accumulation record from the GISP2 core as an indicator of climate change throughout the Holocene. *Science*, **266**, 1680–1682.
- Miller, C. D., 1973, Chronology of neoglacial deposits in the northern Sawatch Range, Colorado. *Arc. Alp. Res.*, **5**, 385–400.
- Nakai, N. and Hong, S., 1980, Climatic changes revealed by geochemical methods on deposits of Lake Yeonglang, South Korea. *Environmental changes in South Korea, Preliminary report of the overseas scientific researches*, 57–61.
- Nakai, N. and Koyama, M., 1987, Reconstruction of paleoenvironment from the viewpoints of the inorganic constituents, C/N ratio and carbon isotopic ratio in the 1400 m core taken from Lake Biwa. In Horie, S., ed., *History of Lake Biwa*. Kyoto Univ. Contrib. **553**, 137–156.
- Omachi City Office, 1983, Preservation of the natural condition of Nishina Three Lakes and the surrounding river system. *Omachi City Office*, 157 p.*
- Ono, R., Kumon, F., Kobayashi, M. and Sakai, J., 2000, Late Quaternary sediments around Lake Aoki, Nagano, central Japan, and the origin of the Lake. *Quatern. Res.*, **39**, 1–13.**
- Ota, Y., Matsushima, Y. and Moriwaki, H., 1982, Notes on the Holocene sea-level study in Japan—on the basis of "Atlas of Holocene sea-level records in Japan". *The Quatern. Res.*, **21**, 133–143.**
- O'Brien, S. R., Mayewski, P. A., Meeker, L. D., Meese, D. A., Twickler, M. S. and Whitlow, S. I., 1995, Complexity of Holocene climate as reconstructed from a Greenland ice core. *Science*, **270**, 1962–1964.
- Park, H. D., Iwami Chi, Watanabe, M. F., Harada, K. and Okino, T., 1998, Temporal variabilities of the concentration of intra- and extracellular microcystin and toxic microcystis species in a hypertrophic lake, Lake Suwa, Japan (1991–1994). *Environ. Toxicol. Water Qual.*, **13**, 61–72.
- Petit-Maire, N. and Bouysse, P., 2000, Geological records of the recent past, a key to the near future world environments. *Episodes*, **23**, 230–246.
- Rind, D. and Overpeck, J., 1993, Hypothesized causes of decade-to-century-scale climate variability : climate model results. *Quatern. Sci. Rev.*, **12**, 357–374.
- Saijo, Y., 2001, Geography. In Saijo, Y. and Hayashi, H., eds.,

- Lake Kizaki*, Backhuys Publishers, Leiden, The Netherlands, 3-11 p.
- Sakaguchi, Y., 1983, Warm and cold stages in the past 7600 years in Japan and their global correlation- especially on climatic impacts to the global sea level changes and the ancient Japanese history. *Bull. Dept. Geogr. Univ. Tokyo*, **15**, 1-31.
- Sakaguchi, Y., 1993, Climate change during the past 8000 years in relation to human history. *Mem. Culture Senshu Univ.*, **51**, 79-113.*
- Stine, S., 1994, Extremes and persistent draught in California and Patagonia during Medieval time. *Nature*, **369**, 546-549.
- Stoermer, E.F. and Ladewski, T.B., 1976, Apparent optimal temperatures for the occurrence of some common phytoplankton species in southern Lake Michigan. *Great Lakes Research Division, Publ. 18, University of Michigan, Ann Arbor*, 47 p.
- Stuiver, M., Reimer, P.J., Bard, E., Beck, W., Burr, G.S., Hughen, K.A., Kromer, B., McCormac, G., Plicht, J.V.D. and Spurk, M., 1998, Intcal98 radiocarbon age calibration, 24000-0 cal BP. *Radiocarbon*, **40**, 1041-1083.
- Sugihara, Y. and Yamanaka, S., 1992, The relationship between environmental changes and Japanese rice yield since the latter half of Little Ice Age. In Mikami, T., ed., *Proc. Int. Symp. on Little Ice Age Climate*, 202-207.
- Talma, A.S. and Vogel, J.C., 1992, Late Quaternary paleotemperatures derived from a speleothem from Congo Caves, Cape Province, South Africa. *Quatern. Res.*, **37**, 203-213.
- Tanaka, A., 1930, *Limnological studies of the lakes in the northern part of Japanese Alps*. Kokin Shoin, Tokyo, 1036 p.*
- Tilman, D. and Kiesling, R.L., 1984, Freshwater algal ecology : taxonomic trade-offs in the temperature dependence of nutrient competitive abilities. In Klug, M. J. and Reddy, C. A., eds., *Proc. of the 3rd Int. Symp. on Microbial Ecology, Michigan State University*, 314-324.
- Umitsu, M., 1976, Geomorphic development of Tsugaru Plain in the Holocene period. *Geogr. Rev. Japan*, **49**, 714-735.**
- Wang, F.B. and Fan, C.Y., 1987, Climatic changes in the Qinghai-Xizang (Tibetan) region of China during the Holocene. *Quatern. Res.*, **28**, 50-60.
- Watanabe, Y., Okino, T. and Sakurai, Y., 1987, Evaluation and discussion of the target level and curtailment of pollutant load for conserving the water quality in Nishina Three Lakes. *Bull. Environ. Conserv. Shinshu Univ.*, **9**, 34-49.
- Xiao, J., Inouchi, Y., Kumai, H., Yoshikawa, S., Kondo, Y., Liu, T. and An, Z., 1997, Biogenic silica record in Lake Biwa of central Japan over the past 145,000 years. *Quatern. Res.*, **47**, 277-283.
- Yamashita, N., Kosaka, T. and Yano, K., 1985, Collapse deposits of the Sanozakayama Hills on the North Coast of Lake Aoki, Nagano Prefecture. *Jour. Fac. Sci. Shinshu Univ.*, **20**, 199-220.**
- Yoshikawa, S., 1983, Volcanic ash layers in the Osaka and Kobiwako Groups, Kinki District, Japan. *Jour. Geosci. Osaka City Univ.*, **27**, 1-40.
- Zhou, S.Z., Chen, F.H., Pan, B.T., Cao, J.X., Li, J.J. and Derbyshire, E., 1991, Environmental changes during the Holocene in western China on a millennial time scale. *The Holocene*, **1**, 151-156.

* : In Japanese, ** : In Japanese with English abstract.

(要 旨)

D.P. Adhikari, F. Kumon and K. Kawajiri, 2002, Holocene climate variability as deduced from the organic carbon and diatom records in the sediments of Lake Aoki, central Japan. *Jour. Geol. Soc. Japan*, 108, 249-265. (ダンダ パニ アディカリ・公文富士夫・川尻 潔, 2002, 中部日本, 青木湖湖底堆積物の有機炭素と珪藻の記録からみた完新世の気候変動. 地質雑, 108, 249-265.)

青木湖は北アルプスの山麓, 標高 822 m にある貧栄養湖である. 表層堆積物の粒度分布を検討し, 1954 年以降の電源開発のための人為的水利用が堆積物の性質と堆積速度に大きな影響を与えていることを明らかにした. 青木湖の北東部から採取した 2.2 m 長のコア試料は, おもに粘土質シルトから構成されており, 年代的には約 1 万年間をカバーしていた. この柱状試料中の有機炭素・窒素含有率と珪藻殻含有数の増減はよく一致しており, 湖の生物生産性の増減が有機炭素・窒素含有率の増減に反映している. 1954 年以前の青木湖の生物生産性は, 気温と連動した水温の変化に支配されていた可能性が高いため, 有機炭素含有率の時代的変遷を基にして完新世の気候変動を復元することができた. 完新世にはそれぞれ 5 つの温暖・冷涼期と 1 つの変動期が認められた. それらの多くは, 小氷期, 中世温暖期, 完新世最温暖期などの汎世界的な寒暖変動とほぼ一致する.